

Understanding the Impact of Gamma Irradiation on Electrical and Mechanical Properties of Epoxy Nanocomposites

R. Karpagam,¹ R. Sarathi,¹ Toshikatsu Tanaka²

¹Department of Electrical Engineering, IIT Madras, Chennai 600 036, India

²IPS Research Center, Waseda University, Kitakyushu, Japan

Received 24 June 2011; accepted 9 September 2011

DOI 10.1002/app.35614

Published online 20 December 2011 in Wiley Online Library (wileyonlinelibrary.com).

ABSTRACT: In this work, the influences of gamma irradiation on the electrical and mechanical properties of the epoxy nanocomposites were studied. The exfoliation characteristics of epoxy nanocomposite material analyzed through TEM studies. It is shown that the impact and flexural strength of the material is high with epoxy nanocomposites and gets reduced with the gamma-irradiated specimen. The AC breakdown strength of the epoxy nanocomposites is high compared with the base epoxy resin. It is also observed that a reduction in permittivity and $\tan(\delta)$ of epoxy resin added with 1 wt % of nanoclay. Increase in percentage of clay shows increase in permittivity and $\tan(\delta)$. Gamma irradiation of epoxy nanocomposite material shows increase in permittivity. The volume resistivity of the material is high with epoxy nanocomposite and is less with gamma-irradiated specimen compared with virgin specimen. The impact strength and flexural strength

indicates correlation with breakdown strength of the material. It is observed that the increase in applied voltage shows an increase in magnitude of the charge density in the insulation structure. With the gamma-irradiated specimen, the charge density (for the applied electric field) is less compared with the virgin specimen. Electric field analysis indicates that the electric field is uniform in the bulk volume of the epoxy nanocomposite material. The rate of charge decay is high with gamma-irradiated specimen compared with virgin specimen. It is realized that material with lower resistivity has faster decay of stored charge. © 2011 Wiley Periodicals, Inc. *J Appl Polym Sci* 125: 415–424, 2012

Key words: nanocomposites; epoxy resin; permittivity; breakdown; resistivity; insulation; space charge; gamma irradiation

INTRODUCTION

Polymer nanocomposites are emerging as a new class of materials for its demanding applications as insulating material in power equipments.^{1,2} Nanocomposites are named when the disperse phase particle size is less than 100 nm.³ Reinforcement of polymeric resin with nanoclay platelets as fillers has resulted in light weight materials with increased modulus and strength, decreased permeability, less shrinkage, and increased heat resistance.⁴ Epoxy resin is an indispensable material for insulation systems in power equipments like dry type transformers and rotating machines.^{5–9} The epoxy resin is used not only as insulating material but also as structural material because the material is cost-effective. It is believed that consistent improvements in properties of clay loaded polymeric system can be achieved by minimizing clay aggregation, promoting the formation of chemical bonds between polymer and clay and achieving exfoliation of clay. It has

been pointed out by other researchers, that the chemical structure of polymer is changed as a consequence of the irradiation through mechanisms like chain scission, oxidation and crosslinking,¹⁰ which results in variation in charge trap behavior.^{11,12} The researchers in the world over are trying to understand the space charge variation due to ageing of insulating material in radioactive environment and the database is scanty.

Having known all this, in this work, a methodical experimental study was carried out, to understand the impact of ageing of epoxy nanocomposite material due to gamma irradiation through certain electrical (breakdown voltage test, volume resistivity, permittivity of the material and $\tan(\delta)$) and mechanical tests (impact and flexural strength of the material). The dispersion of nanoclay in epoxy resin analyzed through transmission electron microscopic (TEM) study. The space charge variations in epoxy nanocomposites, due to ageing, studied by adopting pulsed electroacoustic emission technique.

Correspondence to: R. Sarathi (rsarathi@iitm.ac.in).

EXPERIMENTAL STUDIES

Epoxy nanocomposite synthesized by mechanical shear mixing of organo clay in the resin bath at

TABLE I
Properties of Clay Particle

Color	Off white
Bulk density g/cc	1.5–1.7
Weight loss at 1000°C	37%
D spacing at d_{001}	17.2

room temperature. The clay mineral used in this study was organophillic montmorillonite (MMT) procured from southern clay products (Gonzales, TX) under the trade name of claytone-II. MMT clay is a dry powder that consists of 46.4 wt % of organic compound. The cationic surfactant is $[\text{CH}_3(\text{CH}_2)_n]_2\text{N}(\text{CH}_3)_2$ with components $n = 17, 15,$ and 13 mixed by weight in ratio $65 : 30 : 5$. Claytone II contains organophillic groups of quaternary alkyl ammonium ion. Table I shows the physical properties of claytone-II.¹³ High-speed Shear mixer (which rotates at near 4000 rpm) is used for mixing of clay particles in epoxy resin (DGEBA, CY205, ceba geigy). The shear mixing was carried out for 6 h. The shear mixer generates the shear force to exfoliate/intercalate the clay with uniform dispersion in epoxy resin. Then the sample is mixed with the 4 wt % triethylenetetraamine (TETA) hardner at room temperature for few minutes and the solution is left for degassing. After degassing, the solution is casted in to a sheet of required thickness. After 48 h, the

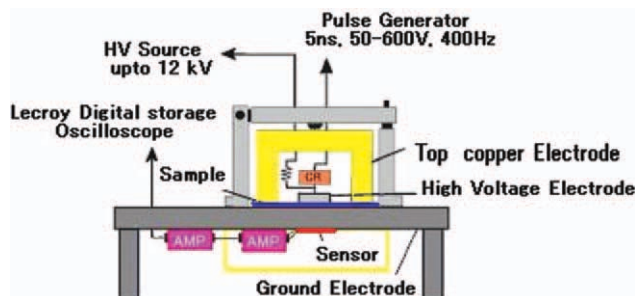


Figure 1 Typical pulsed electroacoustic system. [Color figure can be viewed in the online issue, which is available at wileyonlinelibrary.com.]

prepared samples were used for the study without any further processing. Epoxy nanocomposites with different percentage of clay (~ 1 – 10 wt %) were prepared. The epoxy nanocomposites were exposed to gamma irradiation with a dose rate of 450 kRads/h. In this study, the specimens were exposed to 500, 1000, and 2000 kRads.

The breakdown strength of the material is obtained by placing the 1-mm thick epoxy nanocomposite between two identical spheres on 1.5-cm diameter immersed in transformer oil. The voltage is applied at the rate of 300 V/s. The voltage at which the breakdown occurs at the point of its contact with the electrode considered as the breakdown. The breakdown

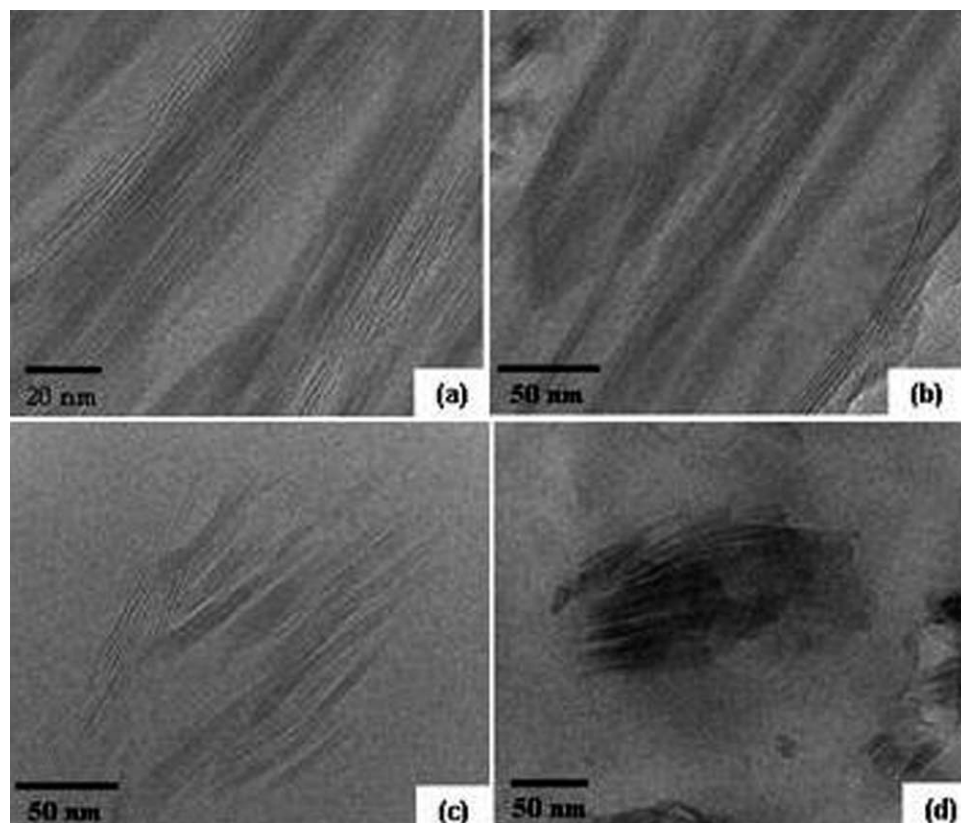


Figure 2 TEM patterns of epoxy nanocomposites: (a) 1% clay, (b) 3% clay, (c) 5% clay, and (d) 10% clay.

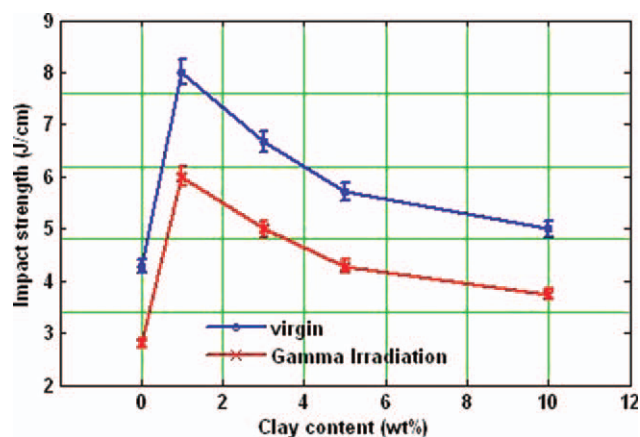


Figure 3 Variation in impact strength due to different percentage of clay in epoxy nanocomposites and with gamma ray (dosed with 2000 kRad) irradiated specimens. [Color figure can be viewed in the online issue, which is available at wileyonlinelibrary.com.]

voltage is calculated based on the average value of the breakdown voltage obtained by conducting test with six specimens.

The ability of a material to resist deformation under a load is its flexural strength. The test was carried out in the universal testing machine of Instron 4301 of 500 kg capacity. The pulling speed during the test is maintained at 5 mm/min. The impact test was carried out in the Frank model machine of 50 J maximum capacity. Here, the impact test is carried out to understand the variation in the material properties of the gamma-irradiated epoxy nanocomposites. The permittivity, $\tan(\delta)$, and volume resistivity of the material were measured using the impedance analyzer (Hioki, Japan Model No.).

The PEA measurement device (Five Lab Make, Japan) was used for the space charge measurement. Figure 1 shows a typical PEA system. The PEA system consist of a 12 kV high-voltage DC source, 600 V pulsed generator (with a rise time of 5 ns) operating at a frequency of about 400 Hz, high-voltage electrodes, sensor for detection of acoustic signal generated due to applied voltage pulse, amplifier and an oscilloscope. The PTFE material is used as sensor material. The electrode system used is of parallel plane configuration. The top electrode coated with semiconducting (carbon loaded) material and the bottom ground electrode is aluminum material. The thickness of the materials used was measured using a vernier. The oscilloscope used for measurement is Lecroy 500 MHz, with sampling rate of 4 GS/s. The insulating material is of flat type sheet material of about 1-mm thickness.

RESULTS AND DISCUSSION

Figure 2 shows the TEM bright field images of epoxy nanocomposites. The thick dark lines are the cross-

section of the clay layers and gray white portions are the epoxy resin. It is observed that the prepared specimens are intercalated with partial exfoliation [Fig. 2(a–c)]. Figure 2(d) shows that, as the weight percentage of clay content is increased to 10% of epoxy resin, agglomeration of particles are formed and dispersion of clay content is limited. This agglomerated zone can act as charge trap site and could enhance the local electric field causing local damage due to incipient discharges.

Figure 3 shows variation in impact strength of the material with different percentage of clay in epoxy resin. It is observed that the impact strength has increased on addition of 1 wt % of nanoclay to epoxy resin and on further increase in clay content in epoxy resin, a reduction in impact strength is observed. It is also observed that the impact strength of nanocomposite material is much higher than the epoxy resin specimen. Figure 4 shows the flexure strength for epoxy resin filled with different percentage of clay content in it. The strength for the epoxy filled with clay particles has increased when 1 wt % of filler is added with epoxy resin and further addition of clay has decreased the strength of the material but much higher than the strength of the epoxy resin. The reduction in impact strength/flexural strength of the material on inclusion of higher percentage filler content could be due to agglomeration of nanofillers, improper adhesion of filler with base resin and due to formation of voids (defect site) in the epoxy nanocomposites.

Figure 5 shows variation in permittivity and $\tan(\delta)$ of the epoxy nanocomposites and for gamma-irradiated specimen. It is observed that the permittivity of the material lies in the range of 3–4 for the virgin and the gamma-irradiated specimen. It is observed

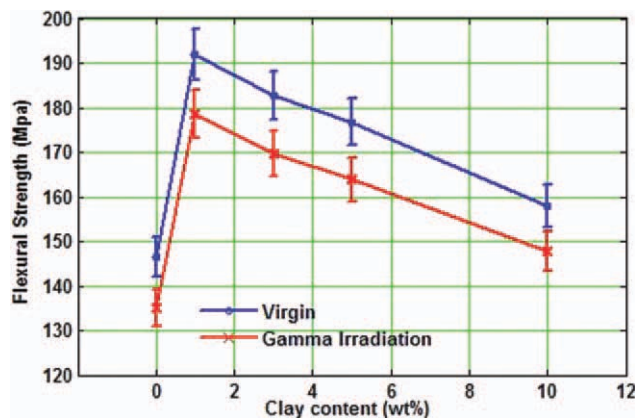


Figure 4 Variation in flexural strength due to different percentage of clay in epoxy nanocomposites and with gamma-irradiated (dosed with 2000 kRad) specimen. [Color figure can be viewed in the online issue, which is available at wileyonlinelibrary.com.]

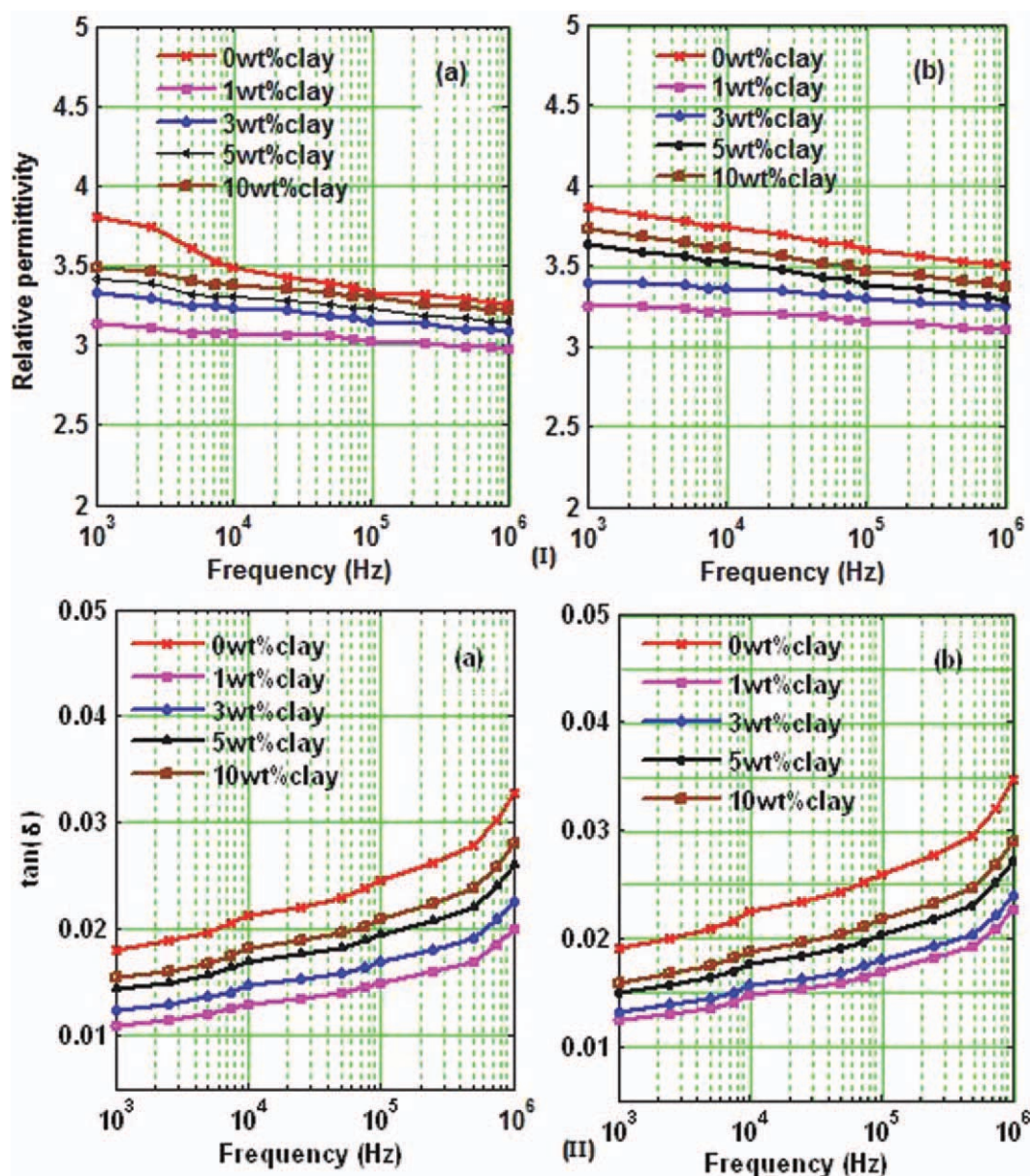


Figure 5 Variation in (I) permittivity and (II) $\tan(\delta)$ of epoxy nanocomposites at different frequencies: (a) virgin and (b) gamma ray irradiated (dosed with 2000 kRad). [Color figure can be viewed in the online issue, which is available at wileyonlinelibrary.com.]

that the permittivity of the gamma-irradiated specimen is high compared with the virgin specimen at lower frequencies. When the supply voltage frequency is increased the permittivity of gamma-irradiated specimen shows reduction in permittivity of the material and such variation is less with the virgin specimen. When increasing the filler content, the material properties overshadow the structural changes and the permittivity increases.¹⁴ Wang indicated that increase in size of the filler shows increase in permittivity of the material.¹⁵ In general, in this study, it is observed that increase in supply frequency shows reduction permittivity of the material.

The $\tan(\delta)$ of the epoxy nanocomposites increases with increase in supply frequency. It is also observed that gamma-irradiated specimens have higher $\tan(\delta)$, compared to the virgin specimen (irrespective of percentage of clay content in epoxy resin). It is also noticed that addition of 1% of clay content in epoxy resin shows drastic reduction in $\tan(\delta)$ of the specimen and on increasing the clay content, shows increase in $\tan(\delta)$ but much lower than the epoxy resin material. This characteristic is observed even with the gamma-irradiated specimen. The value represented here is an average value of six specimens, and it is observed that the scatter in the data is less than 3% of the mean value.

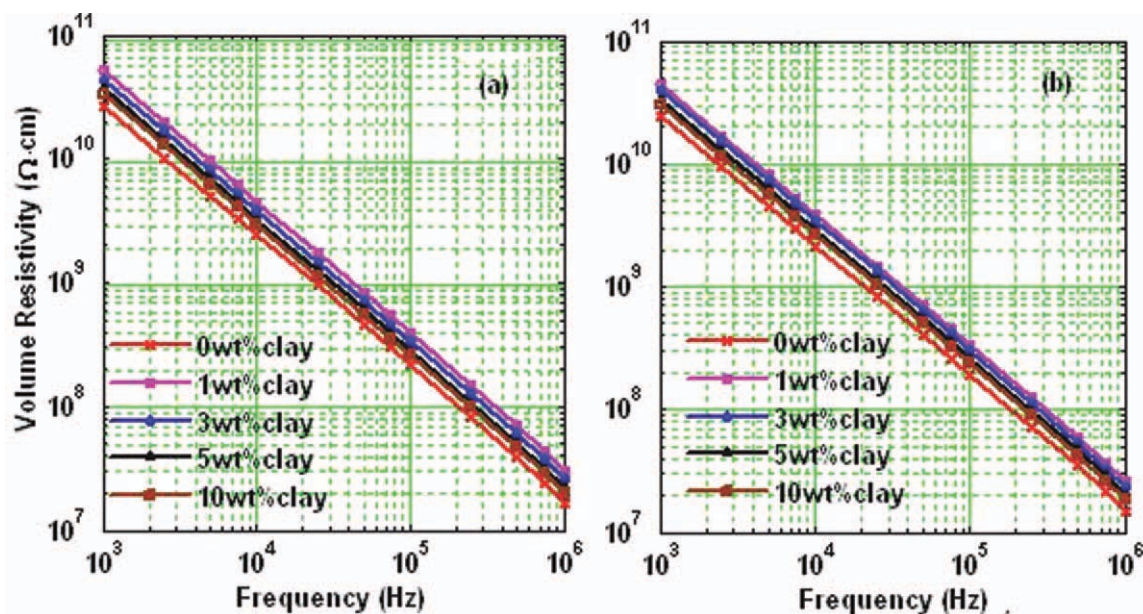


Figure 6 Variation in volume resistivity of the epoxy nanocomposite material: (a) virgin specimen and (b) gamma-irradiated specimen (dosed with 2000 kRad). [Color figure can be viewed in the online issue, which is available at wileyonlinelibrary.com.]

Figure 6 shows variation in volume resistivity of the virgin and the gamma-irradiated epoxy nanocomposite material. It is observed that addition of nanoclay in epoxy resin material shows increase in resistivity of the material. It is observed that increase in supply frequency shows reduction in volume resistivity of the material. Also the resistivity is less with the gamma-irradiated specimen compared with virgin specimen.

Figure 7 shows variation in breakdown strength of the epoxy nanocomposite material. It is observed an increase in breakdown strength of the material with an addition of 1 wt % of clay in epoxy resin. On further increase in clay content in epoxy resin, a marginal reduction in breakdown strength is observed but its value is much higher than the base epoxy resin. Vouyovitch et al. studied breakdown characteristics of service aged epoxy-inorganic particle composites insulator and have concluded that dielectric strength of the material is reduced only by 10% indicating the structural stability of the material. They have suggested that, under quasi-uniform field condition, the electrical field associated to electrical breakdown is calculated as $\beta \times E_m$, where E_m is the ratio between the applied voltage and the thickness of the insulating material and β is the non-uniformity coefficient.¹⁶ In this study, to understand the breakdown characteristics of insulating material, quasi-uniform electric field configuration is used. Because of various percentages of clay content in the epoxy resin, depending on intercalation/exfoliation conditions of clay in epoxy resin, type of hardner and due to any local defect caused due to improper

adhesion of nanoclay with base resin, the breakdown voltage varies. Hence the breakdown voltage was calculated based on average of six breakdowns. It is realized that the scatter in the data is less than 3% of the average and hence the mean breakdown voltage is shown.

In general, the cause for increase in breakdown strength of the epoxy nanocomposite material can be due to increase in surface area of the nanofiller, which may inhibit the charge injection in to the bulk volume forming space charge, leading to increase in breakdown strength of the material. Correlating the impact strength of the material (Fig. 3) and flexural

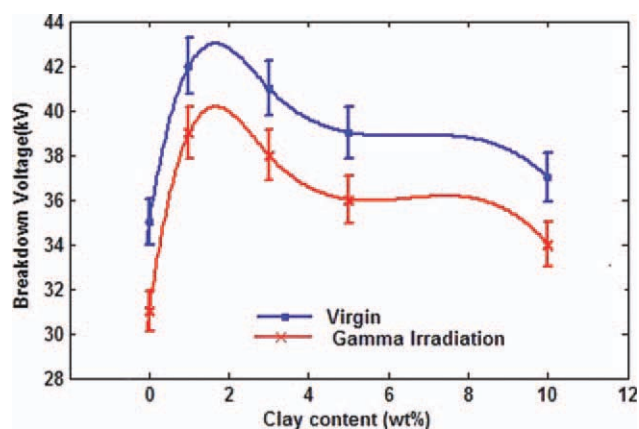


Figure 7 Variation in breakdown strength of epoxy nanocomposites and for gamma ray irradiated specimen (dosed with 2000 kRad). [Color figure can be viewed in the online issue, which is available at wileyonlinelibrary.com.]

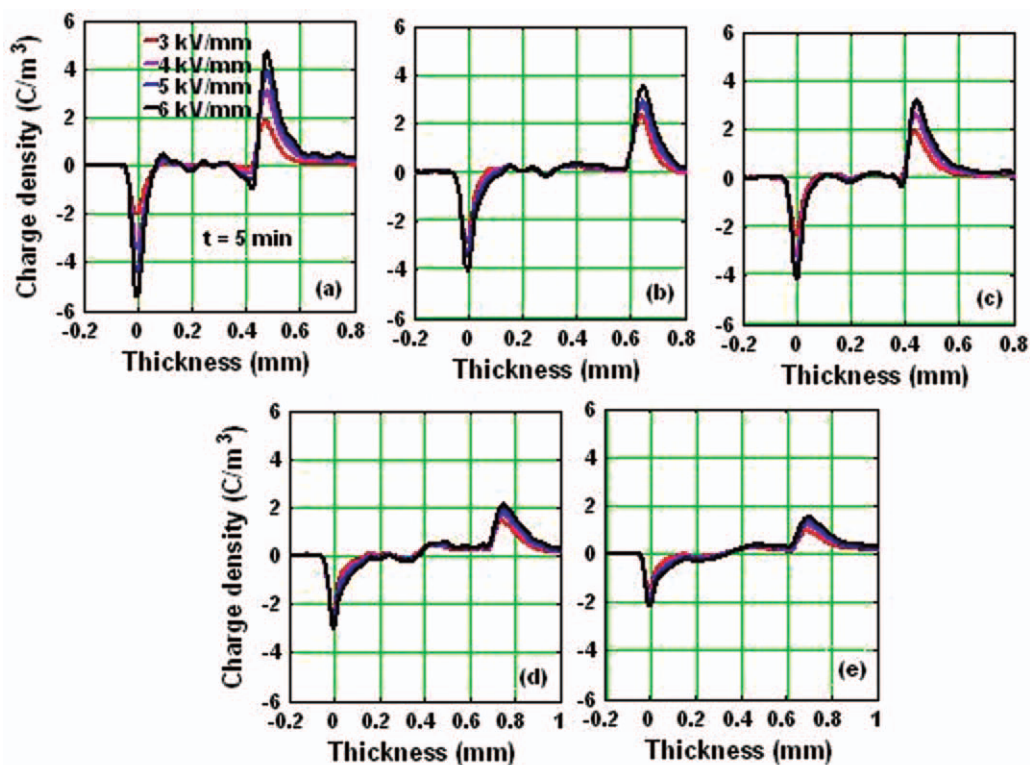


Figure 8 Variation in charge density in epoxy nanocomposites under different voltages: (a) virgin, (b) 1% nanocomposite, (c) 3% nanocomposite, (d) 5% nanocomposite, and (e) 10% nanocomposite. [Color figure can be viewed in the online issue, which is available at wileyonlinelibrary.com.]

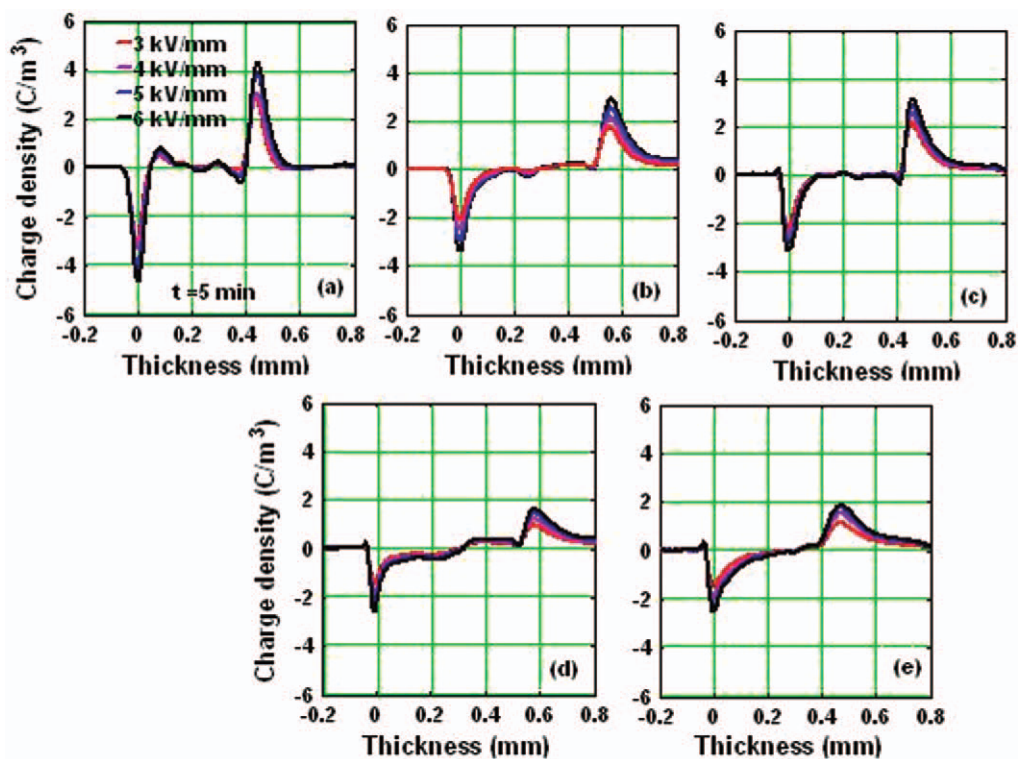


Figure 9 Variation in charge density in gamma ray irradiated (dosed with 2000 kRad) epoxy nanocomposites under different voltages: (a) virgin, (b) 1% nanocomposite, (c) 3% nanocomposite, (d) 5% nanocomposite, and (e) 10% nanocomposite. [Color figure can be viewed in the online issue, which is available at wileyonlinelibrary.com.]

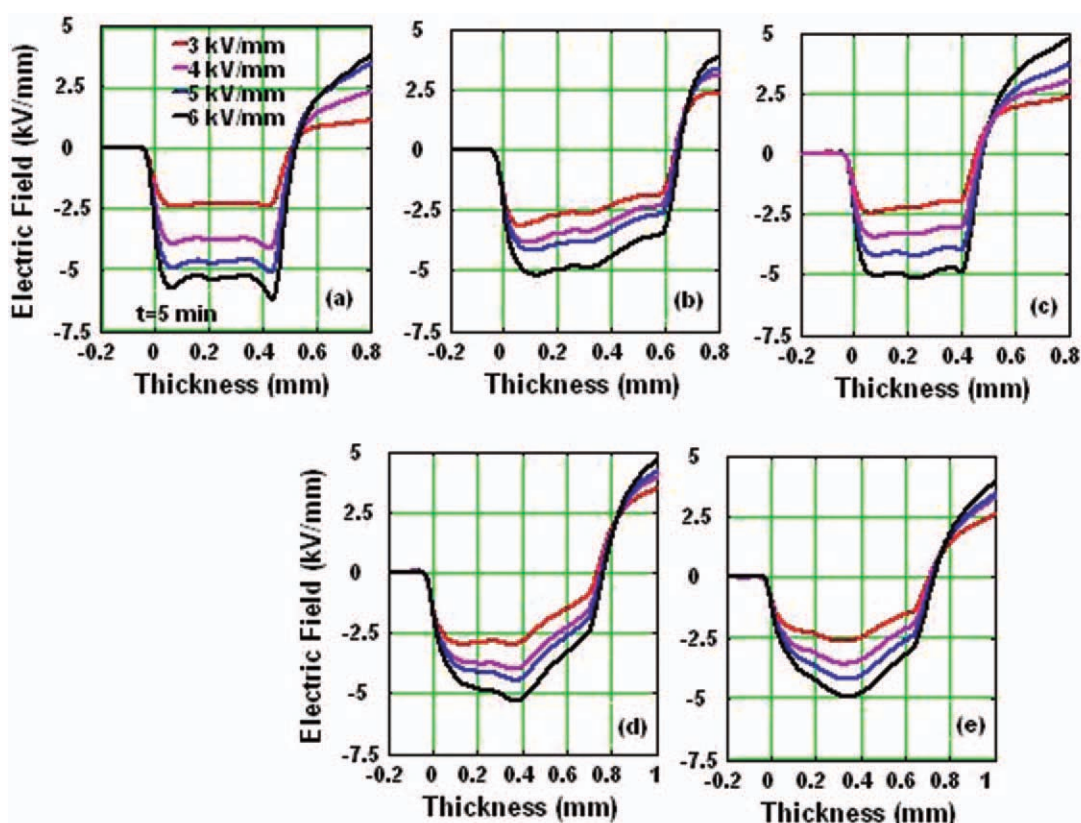


Figure 10 Variation in electric field in epoxy nanocomposite specimens at different voltages: (a) virgin, (b) 1% nanocomposite, (c) 3% nanocomposite, (d) 5% nanocomposite, and (e) 10% nanocomposite. [Color figure can be viewed in the online issue, which is available at [wileyonlinelibrary.com](http://www.wileyonlinelibrary.com).]

strength of the material (Fig. 4) with the breakdown strength of the material, it allows one to conclude that breakdown strength be high when the impact strength and the flexural strength of the material is high (indicating that the material is free from defect).

Figure 8 shows space charge distribution in epoxy nanocomposite material under DC voltages with time. Homocharges are observed near to the electrode, which are considered to be due to charge injection from the electrodes. From Figure 8, it is observed that, in pure epoxy resin specimen certain amount of heterocharges observed near and the bulk volume of insulation. Such characteristics were not observed with the nanocomposite material, irrespective of percentage of clay in epoxy nanocomposites. When the percentage of clay is increased, it is observed that the homocharges accumulates more near to the electrode. Also it is observed that with small amount of percentage of clay in epoxy resin, the space charge magnitude is less compared to pure epoxy resin material and it increases with increase in percentage of clay in epoxy resin above 5%. The reason for such decrease in magnitude of space charge is either that the nanofiller hinders the charge injection or more hetero charges are generated due to the charge separation process. Tagami

et al. has indicated that the curing agents have strongest effect on space charge behavior. They have mentioned that space charge in bulk volume of insulation also be controlled by nanofillers and its level of dispersion. Also, the OH bonds in the clay form strong hydrogen bonds with OH in the amine-cured samples restricting the orientation of the polar groups.¹⁷

Wang et al. studied the influence of size of nanofillers in epoxy resin on space charge effect and has concluded that the fillers can modify the local electric field in the bulk of the insulation.¹⁸ Magraner et al. studied space charge effect in epoxy resin alumina nanocomposites and have concluded that space charge behavior is predominated by the properties of the host resin.¹⁹ Castellon studied space charge behavior in epoxy nanocomposite and they have observed a reduction in space charge with nanocomposites compared with microfilled epoxy resin.²⁰ In general, since the nanocomposite materials have high-packing density, the accumulated charges are reduced and the space charge of heterogeneous charge is reduced.

Figure 9 shows space charge distribution in the gamma-irradiated specimens. It is observed that space charge density has decreased with the

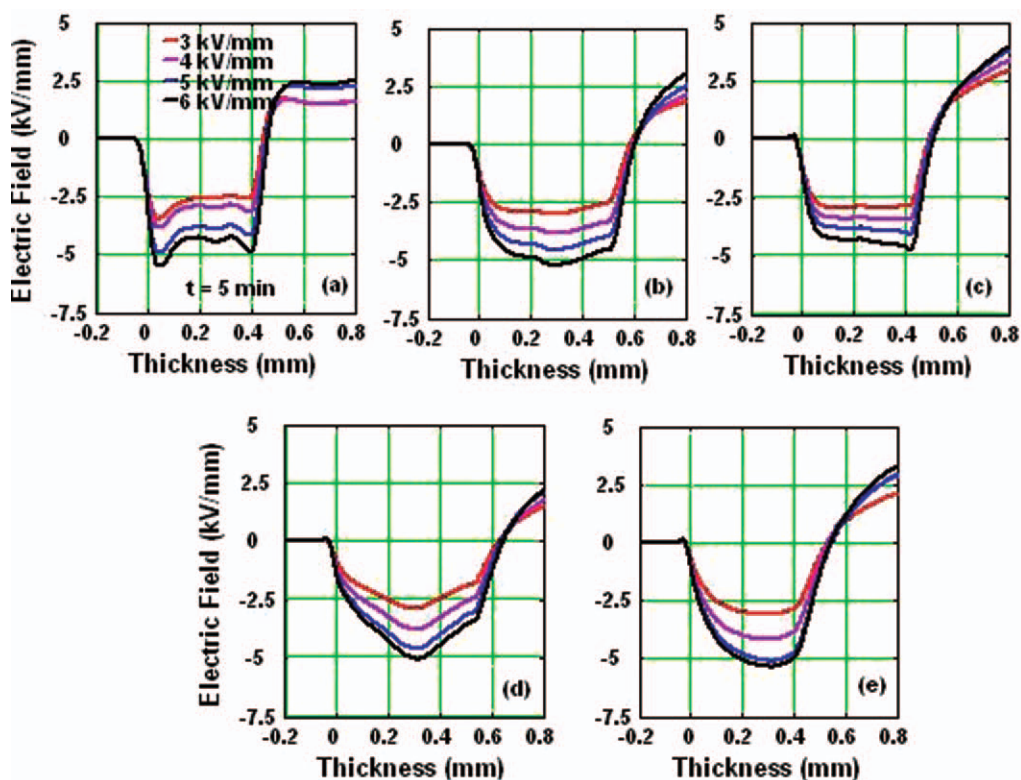


Figure 11 Variation in electric field in gamma ray irradiated (dosed with 2000 kRad) specimens at different voltages: (a) virgin, (b) 1% nanocomposite, (c) 3% nanocomposite, (d) 5% nanocomposite, and (e) 10% nanocomposite. [Color figure can be viewed in the online issue, which is available at wileyonlinelibrary.com.]

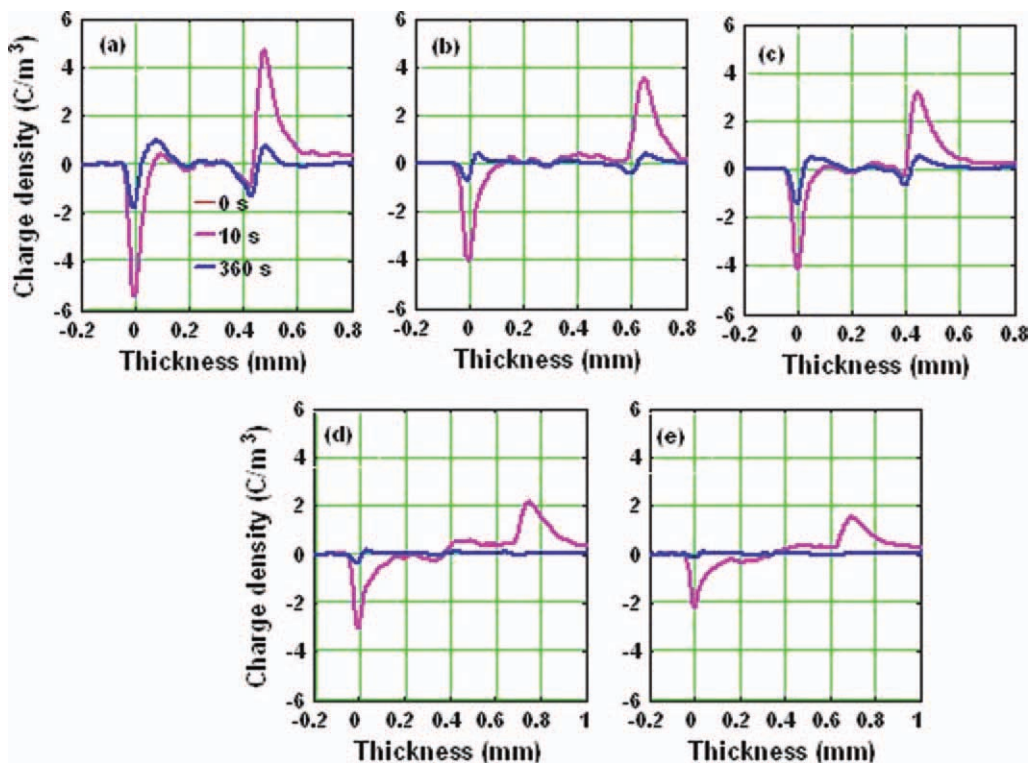


Figure 12 Variation in charge density in epoxy nanocomposite specimens on removal of applied voltage: (a) virgin, (b) 1% clay, (c) 3% clay, (d) 5%, and (e) 10% clay. [Color figure can be viewed in the online issue, which is available at wileyonlinelibrary.com.]

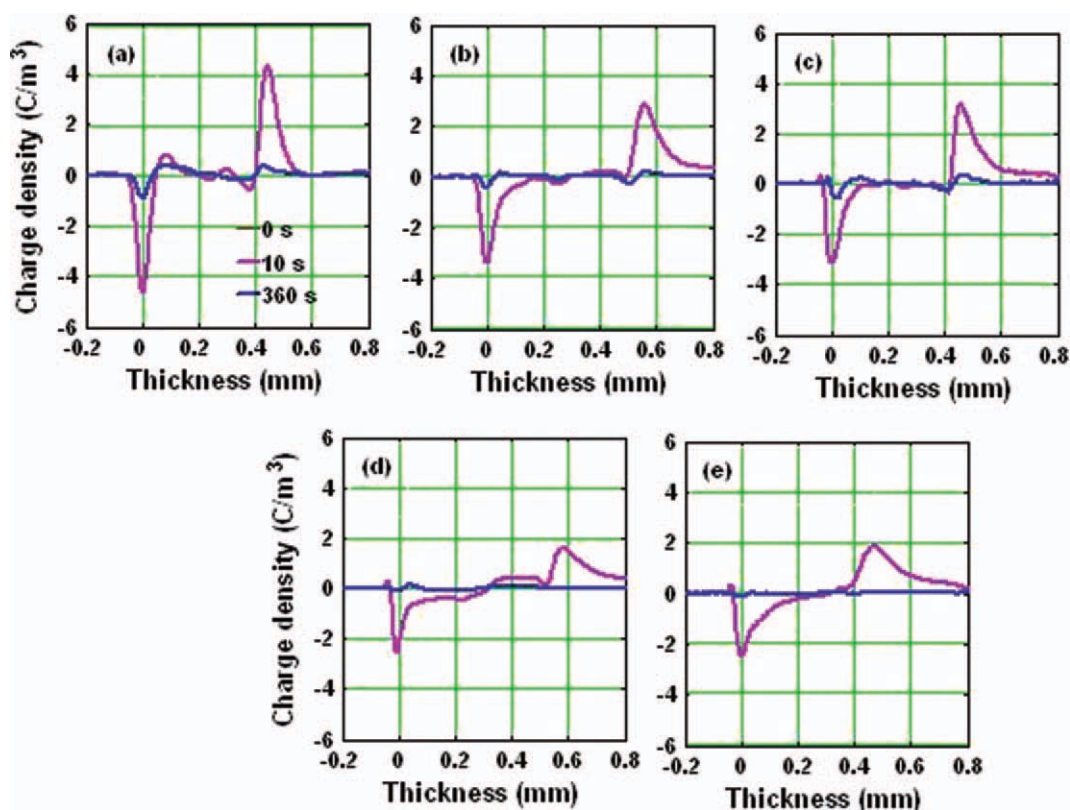


Figure 13 Variation in charge density in gamma ray irradiated (dosed with 2000 kRad) epoxy nanocomposite specimens on removal of applied voltage: (a) virgin, (b) 1% nanocomposite, (c) 3% nanocomposite, (d) 5% nanocomposite, and (e) 10% nanocomposite. [Color figure can be viewed in the online issue, which is available at wileyonlinelibrary.com.]

gamma-irradiated specimen, irrespective of percentage of clay in epoxy resin specimen. The cause for reduction in space charge density with the gamma-irradiated specimen for it could be increase in cross-linking due to gamma irradiation. The amount of injected charge will increase with the electric stress, but equilibrium between charge generation and charge injection achieved after a certain time. In this study, irrespective of level of ageing due to gamma irradiation, the charge accumulation increases linearly with time up to 4 min and then it leveled off. Characteristic variation in space charge density and charge decay process occurs when epoxy nanocomposites were irradiated with gamma rays. During the process of irradiation, hydroxyl group and carbonyl group concentration increases, this introduces shallow trap on the irradiated surface.²¹ When the dosage of gamma irradiation is increased further, more shallow traps that tend to assist the charge migration, which leads to accelerated degradation of the insulating material.

It is well known that space charge can alter the local electric field and can cause reduction in breakdown strength of the material. The electric field could be obtained by integrating the charge profile.²² Figure 10 shows electric field variation in the epoxy nanocomposite material. In this work, it is observed

that electric field enhancement is not observed in the bulk volume of insulation material. Similar characteristics were observed with the gamma-irradiated specimen (Fig. 11).

Figure 12 shows variation in charge decay in the epoxy nanocomposite material on removal of the applied electrical stress. The charge decay in an insulating material is governed by conduction due to electric stress, diffusion due to the concentration gradient, and recombination between the positive and negative charge. It is observed that charge gets decayed fast in epoxy nanocomposite material and with the gamma-irradiated specimen (Fig. 13). Chen et al. studied the space charge behaviors in gamma-irradiated polyethylene material adopting pulsed electroacoustic technique. They have concluded that charge decay is fast with virgin specimen compared with the gamma-irradiated specimen.²³ Similar characteristics are observed with the epoxy nanocomposite material. Comparing the rate of space charge decay on removal of applied voltage (Figs. 12 and 13) and the resistivity of the material (Fig. 6), it indicates that material with lower resistivity have faster decay of stored charge. Admittedly, it has to be mentioned that further work is essential to understand the permissible level of irradiation to epoxy nanocomposite insulating material causing degradation.

CONCLUSIONS

Space charge analysis indicates that homo charges form near to the electrodes in epoxy nanocomposites. TEM analysis indicates that the prepared specimens are intercalated with partial exfoliation. It is observed that the breakdown strength of epoxy nanocomposite is high compared with epoxy resin under AC voltages. A marginal reduction in breakdown strength is observed with the gamma-irradiated epoxy nanocomposite material. Permittivity is high with the gamma-irradiated epoxy nanocomposite material compared with virgin specimen. Also, it is observed that permittivity reduces with increase in supply frequency and the reduction is high with gamma-irradiated specimen. The permittivity of the material reduced when 1 wt % of clay is added to epoxy resin and on increasing the percentage of clay in epoxy resin a marginal increase in permittivity is observed. The Impact strength and flexural strength is high for the epoxy nanocomposite material compared with the virgin specimen. The impact strength and flexural strength of the material shows direct correlation with the breakdown strength of the material. The volume resistivity increases with addition 1 Wt % of nanoclay in epoxy resin. On increasing the percentage of clay in epoxy resin, the volume resistivity reduces but the value has not got reduced much lower than the base epoxy resin material. Volume resistivity of the material reduces with increase in supply frequency. It is observed that the increase in applied voltage shows an increase in magnitude of the charge density in the insulation structure. With the gamma-irradiated specimen, the charge density (for the applied electric field) is less compared with the virgin specimen. Electric field analysis indicates that the electric field is uniform in the bulk volume of the epoxy nanocomposite material. The injected charge decays fast on removal of applied voltage and is high with the gamma-irradiated specimen. It is realized that material with lower resistivity has faster decay of stored charge.

References

1. Tanaka, T.; Montanari, G. C.; Mulhaupt, R. *IEEE Trans Dielectr Electr Insul* 2004, 11, 763.
2. Tanaka, T.; Kozako, M.; Fuse, N.; Ohki, Y. *IEEE Trans Dielectr Electr Insul* 2005, 12, 669.
3. Lewis, T. J. *IEEE Trans Dielectr Electr Insul* 1994, 1, 812.
4. Kozako, M.; Fuse, N.; Ohki, Y.; Okamoto, T.; Tanaka, T. *IEEE Trans Dielectr Electr Insul* 2004, 11, 833.
5. Lan, T.; Pinnavaia, T. *J Chem Mater* 1994, 6, 2216.
6. Pinnavaia, T. J.; Beall, G. W. *Wiley Series in Polymer Science*; New York, 2000.
7. Zilg, C.; Mulhaupt, R.; Finter, J. *Macromol Chem Phys* 1999, 200, 661.
8. Alexandre, M.; Dubois, P. *Mater Sci Eng* 2000, 28, 1.
9. Messersmith, P. B.; Giannelis, E. P. *Chem Mater* 1994, 6, 1719.
10. Chen, G.; Davies, A. E.; Banford, H. M. *IEEE Trans Dielectr Electr Insul* 1999, 6, 882.
11. Das-Gupta, D. K. *IEEE Trans Electr Insul* 1992, 27, 909.
12. Takada, T.; Miyake, H.; Tanaka, Y. *IEEE Trans Plasma Sci* 2006, 34, 2176.
13. Southern Clay Products., Inc., Technical data, Available at: <http://www.scprod.com>.
14. Andritsch, T.; Kochetov, R.; Morshuis, P. H. F.; Smit, J. J. In 10th IEEE International Conference on Solid Dielectrics (ICSD), Potsdam, 2010, pp 1–4.
15. Wang, Q.; Chen, G.; Alghamdi, A. S. In 10th IEEE International Conference on Solid Dielectrics (ICSD), Potsdam, 2010, pp 1–4.
16. Vouyovitch, L.; Alberola, N. D.; Flandin, L.; Beroual, A.; Bessede, J. L. *IEEE Trans Dielectr Electr Insul* 2006, 13, 282.
17. Tagami, N.; Okada, M.; Hirai, N.; Ohki, Y.; Tanaka, T.; Imai, T.; Harada, M.; Ochi, M. *IEEE Trans Dielectr Electr Insul* 2008, 15, 24.
18. Wang, Q.; Curtis, P.; Chen, G. In 2010 Conference on Electrical Insulation and Dielectric Phenomena, Purdue University, West Lafayette, IN, 2010; pp 393–396.
19. Magraner, F.; García-Bernabé, A.; Gil, M.; Llovera, P.; Dodd, S. J.; Dissado, L. A. In 10th IEEE International Conference on Solid Dielectrics (ICSD), 2010, pp 1–4.
20. Castellon, J.; Agnel, S.; Tourelle, A.; Frechette, M. In Annual Report Conference on Electrical Insulation and Dielectric Phenomena, CEIDP, 2008, pp 532–535.
21. Gao, Y.; Du, B. X.; Zhu, X. H. In Annual Report Conference on Electrical Insulation and Dielectric Phenomena, CEIDP, 2009, pp 169–172.
22. Fukunaga, K. *IEEE Electr Insul Mag* 2004, 20, 18.
23. Chen, G.; Davies, A. E. *IEEE Trans Dielectr Electr Insul* 1999, 6, 882.